



ELSEVIER

Available online at [www.sciencedirect.com](http://www.sciencedirect.com)

SCIENCE @ DIRECT®

Sedimentary Geology 181 (2005) 173–194

**Sedimentary  
Geology**

[www.elsevier.com/locate/sedgeo](http://www.elsevier.com/locate/sedgeo)

# Aragonite dissolution, sedimentation rates and carbon isotopes in deep-water hemipelagites (Livinallongo Formation, Middle Triassic, northern Italy)

Nereo Preto <sup>a,\*</sup>, Christoph Spötl <sup>b</sup>, Paolo Mietto <sup>a,c</sup>, Piero Gianolla <sup>d</sup>,  
Alberto Riva <sup>d</sup>, Stefano Manfrin <sup>a</sup>

<sup>a</sup> *Dipartimento di Geologia, Paleontologia e Geofisica, University of Padova, Via Giotto 1, 35137 Padova, Italy*

<sup>b</sup> *Institut für Geologie und Paleontologie, Universität Innsbruck, Innrain 52, 6020 Innsbruck, Austria*

<sup>c</sup> *Istituto CNR di Geodinamica e Georisorse, sez. di Padova, Via Garibaldi 37, 35137 Padova, Italy*

<sup>d</sup> *Dipartimento di Scienze della Terra, University of Ferrara, Corso Ercole d'Este 32, 44100 Ferrara, Italy*

Received 13 June 2005; accepted 3 August 2005

## Abstract

Hemipelagic nodular limestones are a widespread facies in the Triassic of the Tethys, often considered as being deposited at rather constant sedimentation rates. The aim of this paper is to investigate the sedimentation rate variability in a case-study from the Middle Triassic of the Dolomites, northern Italy, and to suggest possible causes. The nodular cherty limestones of the Livinallongo Fm. and correlated units were studied in four stratigraphic sections and compared to classical successions from the literature. Correlations between sections are based on ammonoid biostratigraphy and tephra stratigraphy. Correlation highlighted conspicuous changes in sedimentation rates through time and between sections, associated with sedimentological evidence of deep-water aragonite dissolution. Deep-water dissolution is believed to have resulted in small hiatuses and in a bias of ammonoid assemblages towards taxa with more resistant shells. Carbonate petrography and geochemistry provide evidence of differential diagenesis of the Livinallongo Fm. Carbonate nodules were lithified at the water–sediment interface, and their C isotope composition is regarded as a proxy of the  $\delta^{13}\text{C}$  of Middle Triassic bottom seawater. The onset of nodular cherty limestones, occurring contemporaneously at the basin scale, and the coeval carbonate platform drowning events are tentatively explained by the inflow and local upwelling of cool deep water from Panthalassa into the western Tethys.

© 2005 Elsevier B.V. All rights reserved.

*Keywords:* Middle Triassic; Hemipelagic environment; Sedimentation rates; Carbon isotopes; Tethys; Ocean circulation

## 1. Introduction

Monotonous successions of nodular cherty limestones are a widespread deep-water facies in the Trias-

\* Corresponding author. Tel.: +39 049 827 2092; fax: +39 049 827 2070.

E-mail address: [nereo.preto@unipd.it](mailto:nereo.preto@unipd.it) (N. Preto).

sis of the western Tethys. Well-known examples are the Middle Triassic Livinallongo Fm. of the Dolomites (Viel, 1979), along with the equivalent Buchenstein Beds of Lombardy (Brack and Rieber, 1993), the *Nodosus* Fm. of Recoaro (northern Italy) (De Zanche and Mietto, 1981), the “Buchenstein Formation” of Balaton highlands (Hungary) (Vörös et al., 1996), the Middle to Upper Triassic Reifling Limestones of the Northern Calcareous Alps (Austria), and the “Calcari con Selce” (i.e., cherty limestones) of the Lagonegro basin (Scandone, 1967) and Sicily (Di Stefano, 1990).

This Triassic facies characterizes most deep-water periplatform areas, whereas the condensed red nodular limestones known as “Hallstatt Limestones”, widespread throughout the Tethys margin from Austria to Timor, are probably hemipelagic sediments deposited further away from carbonate platform margins (e.g., Gawlick and Böhm, 2000; Channell et al., 2003). This article focuses on the Middle Triassic Livinallongo Fm., a representative example of the depositional and early diagenetic processes in Triassic periplatform hemipelagites. The sediments of this lithostratigraphic unit underwent differential diagenesis as illustrated by the differential compaction of nodules and surrounding sediment. Due to the deep-water setting and the absence of facies changes, these hemipelagic nodular limestones may be regarded as “background sedimentation” (e.g., Brack and Rieber, 1993; Maurer and Schlager, 2003; Maurer et al., 2003), characterized by a rather constant sedimentation rate. It is notoriously difficult to demonstrate changes in sedimentation rate in such settings, especially where diagnostic sedimentary structures (e.g., hard-grounds, phosphatic concentrations or clearly identifiable omission surfaces) are absent. Within the Livinallongo Fm., however, correlations at the bed scale are possible using marker beds (e.g., Brack and Muttoni, 2000; Muttoni et al., 2004) allowing changes in sedimentation rate to be investigated by comparison of stratigraphically correlated sections.

In this paper, several issues regarding sedimentation rate and early diagenesis of hemipelagic nodular limestones are addressed based on new biostratigraphic, lithostratigraphic, sedimentological and geochemical data from the Middle Triassic Livinallongo Fm. and from the coeval Latemar carbonate platform. Biostratigraphic data, along with the recognition of marker beds, provide a high-resolution correlation framework. Our analysis reveals strong variations in

sedimentation rate both between and within sections, i.e., in space and time. Furthermore, aspects of the early diagenesis of these hemipelagic nodular limestones are unravelled, adding further evidence of differential diagenesis and suggesting that this facies might retain an original geochemical signal of Middle Triassic seawater.

## 2. Geological setting

During the Late Anisian, most of the area of the Dolomites formed an extensive shallow-water carbonate bank (Contrin Fm.) surrounded by basins in the eastern Dolomites (Ambata Fm.) and in Lombardy (Prezzo Lms) (Fig. 1). A subsequent period of extensional tectonics dissected the uniform carbonate bank of the Contrin Fm. into a horst-and-graben topography. Anoxic–dysoxic sediments with carbonate megabreccias (Moena Fm.) were deposited in the grabens (Masetti and Neri, 1980), while the growth of the Contrin carbonates continued on structural highs. Some portions of the surviving Contrin carbonate bank, however, became drowned later (e.g., Masetti and Neri,

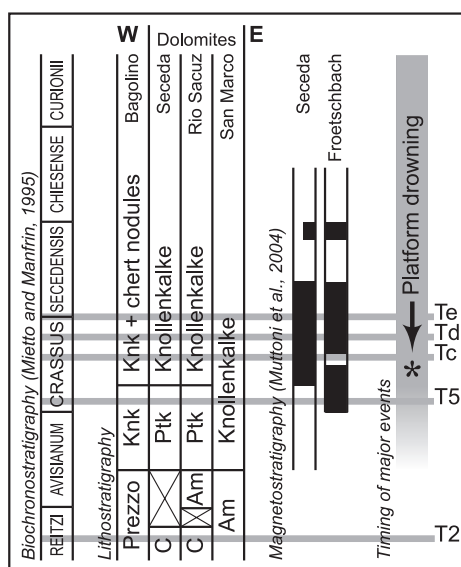


Fig. 1. Outline of the events discussed here, in the framework of the stratigraphy of the Southern Alps. Am: Ambata Formation; C: Contrin Formation (carbonate platform); Knk: Knollenkalke; Ptk: Plattenkalke; T2, T5, Tc, Td, Te: Marker beds (tuffs). The timing of cool water inflow in the Southern Alps, as proposed in this study, is shown by the grey shading.

1980; Brack and Rieber, 1993). The tectonic break-up of the Contrin carbonate bank resulted in a complex topography of shallow and deep areas that influenced the evolution of the Dolomites during the Ladinian and Carnian. Carbonate platforms developed in shallow

seas, whereas the depocenters became the loci of hemipelagic sedimentation. The first basinal formation of the Ladinian is the Livinallongo Fm., which interfingers with carbonate platforms known as “Lower Edifice” (sensu De Zanche et al., 1993) and Sciliar Dm.

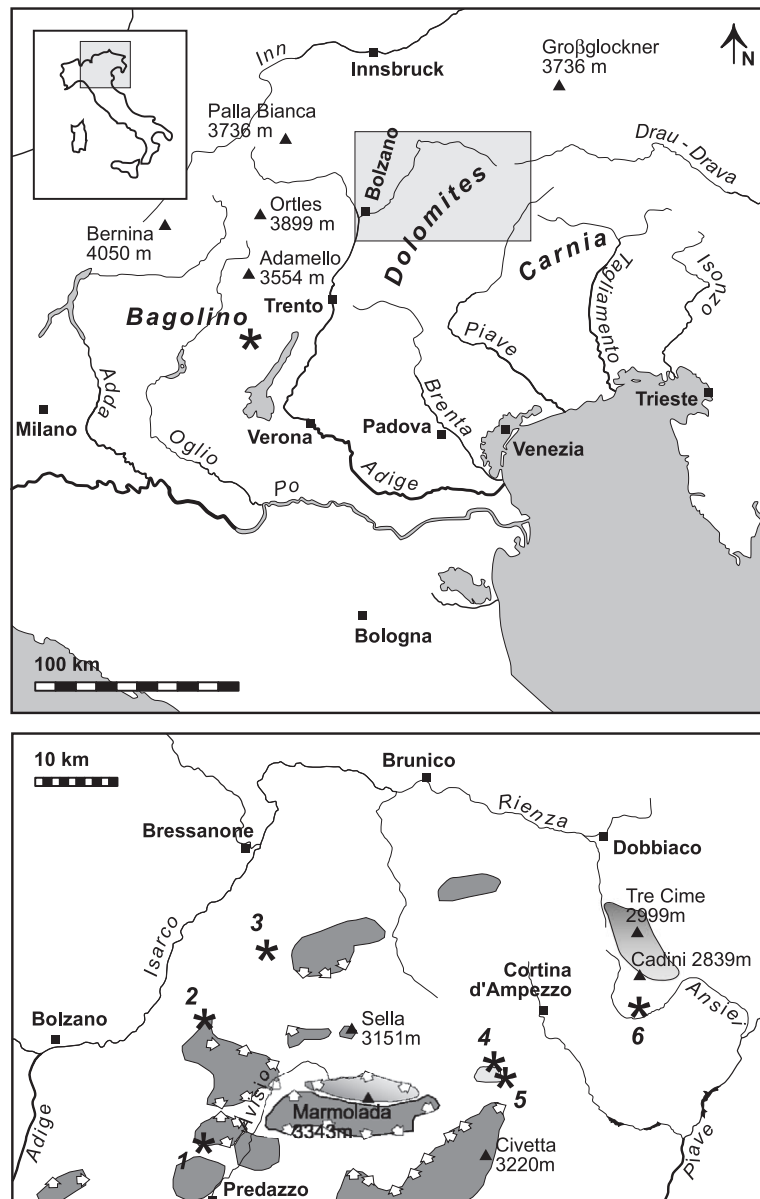


Fig. 2. Map of the study area, with an enlargement of the Dolomites area. 1) Latemar platform; 2) Frötschbach section; 3) Seceda section; 4) Punta Zonia section; 5) Rio Sacuz section; 6) Palus–San Marco section. The location of post-Contrin Late Anisian–Ladinian carbonate platforms is shown in dark grey; partially or completely drowned platforms are shown in light grey. Arrows indicate progradation directions. Alpine deformation was not restored in this map.

The Livinallongo Fm. (Viel, 1979; De Zanche et al., 1993) is a deep-water formation, deposited in rapidly subsiding basins, whose facies are traditionally considered to be rather persistent throughout the region (cf. Brack and Rieber, 1993; Brack and Muttoni, 2000). Following Viel (1979), we use the term “Buchenstein” as the name of a group, within which the Livinallongo Fm. is the lowermost formation. Often, the Livinallongo Fm. sharply overlies Late Anisian dolomitized platform carbonates (Contrin Fm.), and can be subdivided into three members: Plattenkalke, Knollenkalke and Bänderkalke (e.g., Viel, 1979; De Zanche et al., 1993). The Plattenkalke are constituted by black, laminated, siliceous limestones and dolostones rich in organic matter. Knollenkalke consist of greenish-grey, bioturbated nodular limestones, with chert nodules and beds. The Bänderkalke are again characterized by laminated limestones, accompanied by abundant coarse grained turbidite beds. At Seceda (Fig. 2), the boundary between the Plattenkalke and Knollenkalke is sharp (Brack and Muttoni, 2000). Tuffs (i.e., tephra) and volcanoclastic intercalations, locally known as “Pietra Verde”, are common throughout the formation and can be used as marker beds (Brack and Muttoni, 2000). In some localities, the Livinallongo Fm. lies on the basal Ambata Fm., and the Plattenkalke may be absent (e.g., Rio Sacuz and San Marco, Fig. 2).

The nodular facies of the Livinallongo Fm. (Knollenkalke Mb.) are widespread throughout the Southern Alps, and are also found in the Northern Calcareous Alps (Reifling Lms.) and Hungary (“Buchenstein Formation”). The Bagolino section (Fig. 2) is the best exposed and most complete section of the Buchenstein Group in Lombardy. There, the Plattenkalke and Bänderkalke cannot be distinguished and are substituted by Knollenkalke-like facies with tuff and volcanoclastic intercalations; thus, the Knollenkalke account for the equivalent of the entire Livinallongo Fm. At Bagolino, the Knollenkalke rests on the hemipelagic Prezzo Limestone.

### 3. Methods

Stratigraphic sections were measured at the cm scale in the field and carefully investigated to recover a sufficient number of ammonoid specimens that

allowed to establish a reliable ammonoid biostratigraphy. The biostratigraphic scale of Mietto and Manfrin (1995) was preferred due to its high resolution. Special care was taken in the field to recognize turbidites in the hemipelagic successions.

In order to identify the diagenetic evolution that led to lithification of nodules in the Knollenkalke Mb. ca. 70 petrographic thin sections from the San Marco and Rio Sacuz sections were examined. These observations were extended to ca. 200 additional thin sections of Knollenkalke from several localities in the Southern Alps, obtained from collections of the Geological Departments of Padova and Ferrara Universities. A further ca. 200 thin sections from the Latemar platform interior and the Punta Zonia section were also examined, partly during an earlier study (Preto et al., 2001). Twelve selected thin sections were studied using cathodoluminescence (CL) microscopy. The cold-stage CL instrument (CITL CCL 8200 Mk3) at the Institute of Geosciences and Georesources (CNR, Padova) operated at 20 kV beam energy and 200 mA beam current. Chips from five samples were gold-coated and examined using a CamScan MX2500 Scanning Electron Microscope (SEM) at the Mineralogy and Petrology Department of Padova University.

Powders for stable isotope analyses were hand-drilled from slabs of macroscopically homogeneous mudstones. Thin sections of selected samples were subsequently used to confirm that the drilled powders did not include late diagenetic vein calcite. Such calcite veins were also analyzed in samples from Rio Sacuz and San Marco in order to compare their isotopic composition to that of the micrite. Calcite powders were reacted with phosphoric acid and analyzed using an automated continuous-flow isotope ratio mass spectrometer at the University of Innsbruck calibrated against NBS and IAEA standards. Results are reported relative to VPDB scale and the long-term analytical uncertainties reported at the  $1\sigma$  level are 0.07‰ and 0.08‰ for  $\delta^{13}\text{C}$  and  $\delta^{18}\text{O}$ , respectively (Spötl and Vennemann, 2003).

### 4. Studied sections

Four stratigraphic sections were studied, Rio Sacuz, San Marco, Punta Zonia and Cimon del Latemar. The Rio Sacuz (Fig. 2, locality 5) and San Marco (Fig. 2,

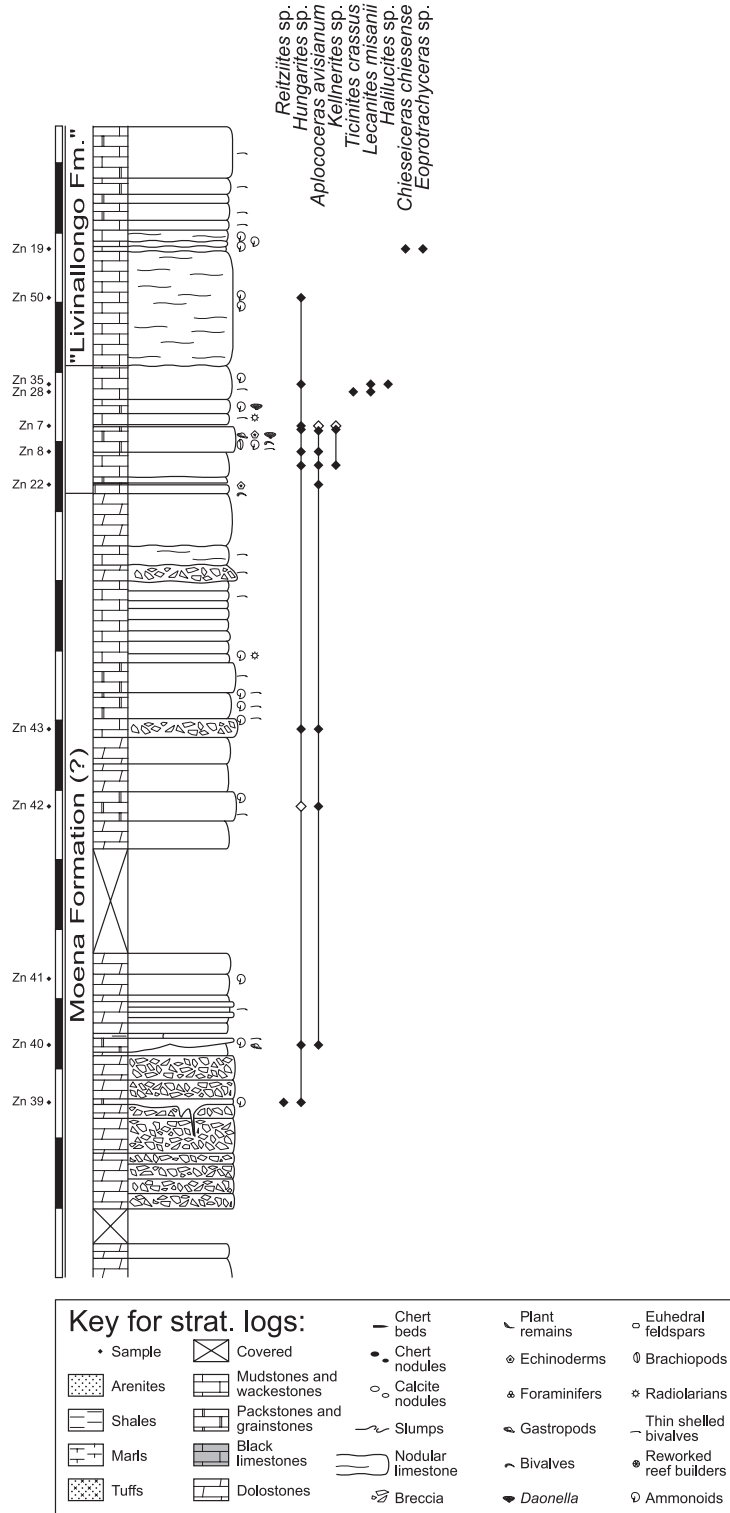


Fig. 3. Punta Zonia section, and distribution of ammonoids. Data partly from De Zanche et al. (1995). 1 m gradations on vertical scale.

locality 6) encompass the Ambata Fm. and the lower to middle part of the Livinallongo Fm. in a basinal setting. Rio Sacuz starts with massive dolostones representing the eastern slope of a carbonate bank equivalent to the Anisian Contrin Fm. found at the classical Seceda section (e.g., Brack and Rieber, 1993; Maurer and Schlager, 2003). The Plattenkalke of Rio Sacuz are ca. 15 m thick, and, contrary to Seceda, overlie ca. 25 m of hemipelagic turbidites (Ambata Fm.) rather than shallow-water carbonates. The change from the black laminated facies of the Plattenkalke to the bioturbated, nodular facies of the Knollenkalke takes place gradually within a 9 m-thick transitional unit composed of light grey limestones alternating with darker, silicified marls. Slumping structures are present throughout the section. These structures, together with the coarse carbonate turbidite beds in the lower part of the Upper Ambata Fm. and the fact that this formation rests directly on a slope indicate that the Rio Sacuz section represents either a distal slope setting or a basinal setting proximal to the slope of the nearby Cenera carbonate platform, in agreement with previous studies (Blendinger et al., 1982; Cros and Vrielynck, 1989).

The best exposed section at San Marco ranges from the Upper Bivera Fm. (Late Anisian) to the Upper Knollenkalke Mb. of the Livinallongo Fm. (Casati et al., 1982). Lithologies comparable to the Plattenkalke are absent. The microfacies of the limestones is remarkably constant throughout the whole section: wackestone–packstones with calcified radiolarians and thin-shelled bivalves, with evidence of pervasive bioturbation. Only few turbidite beds can be recognized in the field. All layers are laterally continuous, and can be traced for at least 200 m along the outcrop. The San Marco section can thus be attributed to a basinal setting, albeit its proximity to a carbonate platform. As far as the sedimentary environment of the Knollenkalke is concerned, the section is closely comparable to the Seceda section.

The third section, Punta Zonia (Fig. 2, locality 4; Fig. 3), crops out on the northern side of the nearby Cenera platform and records its evolution and drowning (Cros and Houel, 1983; De Zanche et al., 1995). Punta Zonia represents the transition from a slope to a hemipelagic sedimentary environment, as indicated by depositional geometries and facies analysis. The base of the section is composed of massive dolostones, belonging to the slope of the Contrin Fm.,

as indicated by tracing of the unit eastwards into a margin and a thicker platform interior. The following 10 m of carbonate breccias, calcarenites, calcirudited, and bituminous dolostones (Moena Fm.) are overlain by intra-bioclastic grainstones and encrinites. These layers contain bioclasts (echinoderms, bivalves, gastropods, brachiopods, foraminifers, along with pelagic fossils such as thin-shelled bivalves and ammonoids) and are succeeded by wackestone–packstones with thin-shelled bivalves, radiolarians and ammonoids, with undulated layering and chert horizons. This unit is strongly affected by stratigraphic condensation in its upper part and is regarded as hemipelagic sedimentation.

The fourth section (Cimon del Latemar) was measured in a platform interior setting. The Latemar platform (Fig. 2, locality 1) is an isolated carbonate buildup characterized by a ca. 600 m-thick platform interior succession, constituted by a monotonous stack of hundreds of peritidal carbonate sedimentary cycles, capped by subaerial exposure horizons (e.g., Goldhammer et al., 1987; Egenhoff et al., 1999). Correlation was possible due to the abundant ammonoids preserved in sedimentary traps within the platform interior (Manfrin et al., 2005).

## 5. Correlations and changes in sedimentation rate

The study sections are correlated by ammonoid biostratigraphy and tephrostratigraphy (Fig. 4). With respect to previous works, two additional tuff markers are considered (T2 and T5 in Mietto et al., 2003b). Their correlation is in good agreement with ammonoid biostratigraphy. Punta Zonia (Fig. 3) lacks correlatable tuffs, and can be correlated with less precision, based only on biostratigraphy.

For the Latemar platform, the correlation of tuffs is only suggested (Fig. 4) based on the assumption that the highest tuff of the Latemar corresponds to Te, which is the highest continuous tuff in the Lower Knollenkalke. This correlation is in excellent agreement with the biostratigraphy of Manfrin et al. (2005).

### 5.1. Lateral variations in sedimentation rate

The sedimentation rate variability of the Livinallongo Fm. or Buchenstein group is still a matter of

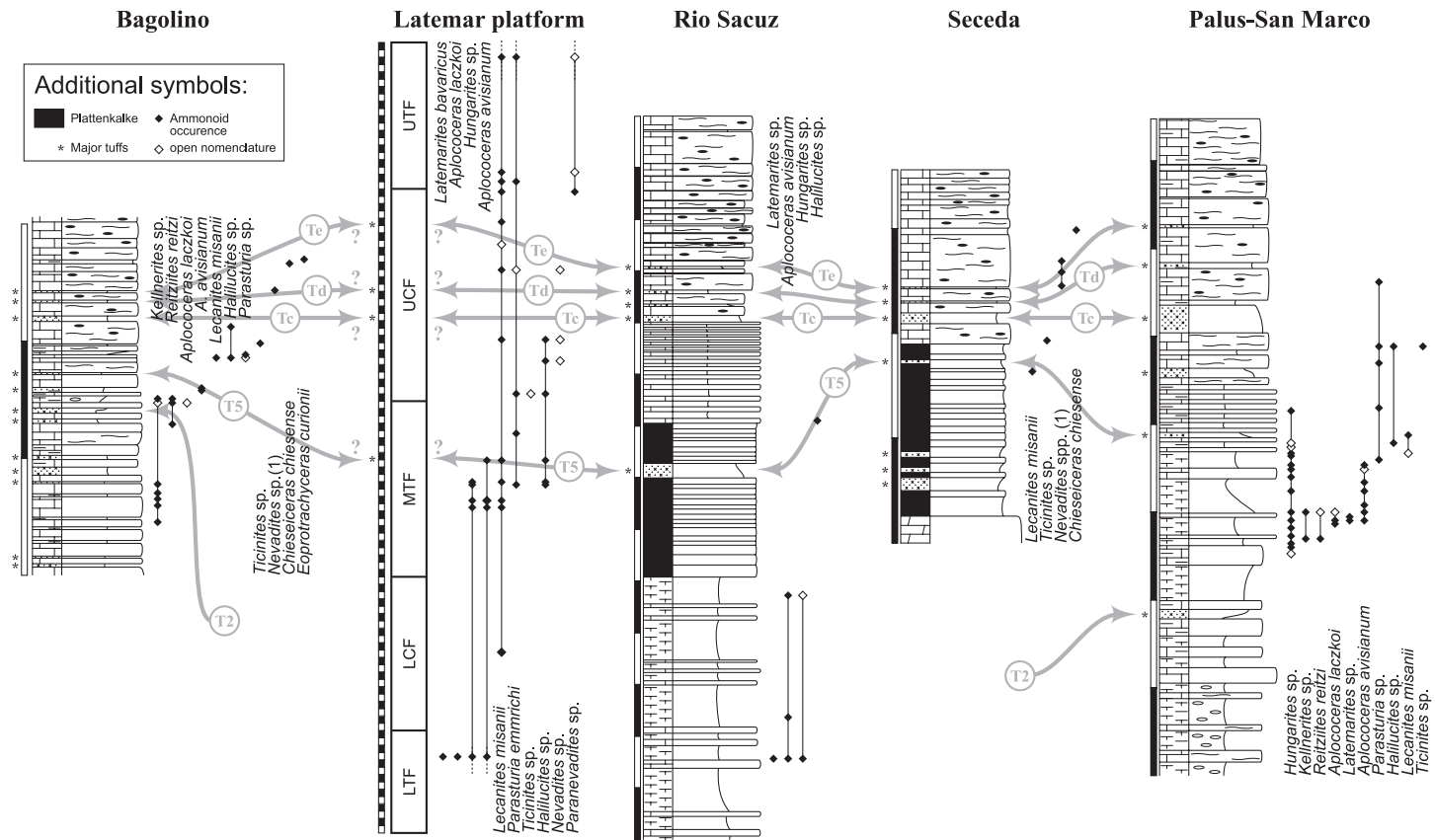


Fig. 4. Simplified logs of correlated sections within the Southern Alps, 5 m gradations on vertical scale, and distribution of selected ammonoid taxa. Legend as in Fig. 3. Grey arrows indicate correlated tuffs (tephras); the stratigraphic position of tuffs in the Latemar platform section is hypothesized (see text). Bagolino: redrawn from Brack and Rieber, 1993; ammonoid distribution from Brack and Rieber, 1993 and Mietto et al., 2003a. Latemar platform: ammonoid distribution from Manfrin et al., 2005. Seceda: redrawn from Brack and Rieber, 1993, who presented a section extended upwards for several meters; ammonoid distribution from Brack and Rieber, 1993 and De Zanche et al., 1995. All other logs and distributions from authors' original data. (1): *Nevadites* sensu Brack and Rieber (1993).

debate (Mietto et al., 2003b); for intervals between individual marker beds, however, an a priori comparison of sedimentation rates can be made between correlated sections (Table 1). A dramatic change in sedimentation rates is observed between the Latemar platform and the basinal series, due to strong synsedimentary subsidence, rapid aggradation of carbonate platforms (the Latemar keeps up easily with the sea-level, as demonstrated by the subaerial exposure surfaces widespread throughout the platform interior succession), and slow sedimentation in the basin. Large variations in sedimentation rates are observed also within the basin itself, especially below the base of the Knollenkalke. Apparently, the roughly synchronous onset of the Knollenkalke facies in the Southern Alps is also accompanied by a levelling out of the sedimentation rates. It is interesting to note that the Bagolino section, GSSP (Global Stratigraphic Section and Point) of the base of the Ladinian, has the lowest sedimentation rates among all studied sections.

### 5.2. Variations of sedimentation rates in time

In order to identify variations of the sedimentation rates through time, three tuffs were selected (T5, Tc, Te) because of their straightforward recognition and lateral continuity. T2 was also considered when present. The stratigraphic interval between Tc and Te was rescaled in each section to the same thickness. We chose to normalize this interval mostly because the carbonate layers between Tc and Te maintain the same facies in all the studied sections.

If the sedimentation rate remained constant in all sections (or, the sedimentation rate varied in the same way in all sections), the proportion of thicknesses between marker beds must be the same in each section, and if one interval is forced to the same rescaled thickness, all others must also result in a uniform (rescaled) thickness between sections. In Table 2,

Table 1

Thicknesses between marker horizons (m)

Section\markers	T2–T5	T5–Tc	Tc–Te
Latemar	=	96	59.5
Rio Sacuz	=	13.7	4.6
San Marco	10.1	5.45	4.4
Seceda core	=	2.75	1.9
Bagolino	1.75	1.25	1.0

Table 2

Thicknesses between markers, after rescaling (dimensionless)

Section\markers	T2–T5	T5–Tc	Tc–Te
Latemar	=	1.61	1
Rio Sacuz	=	3.0	1
San Marco	2.30	1.25	1
Seceda core	=	1.45	1
Bagolino	1.75	1.25	1

the rescaled thicknesses between marker beds are shown. Normalization strongly reduces sedimentation rate contrasts between sections, possibly because differences related to local factors are partly removed by this transformation. Nevertheless, the rescaled thicknesses of the intervals below Tc still show significant variations (Table 2), corresponding to variations of sedimentation rates through time.

## 6. Early diagenetic features of the Knollenkalke

### 6.1. Contemporaneous cementation and dissolution at the water–sediment interface

There is clear evidence that the carbonates of the Knollenkalke were already cemented prior to burial; at the same time, some features can be explained only by aragonite dissolution at the water–sediment interface. Sedimentological features suggesting early lithification and aragonite dissolution include fracturing and reworking of carbonate nodules, occurrence of uncompacted bivalve coquinas, silicification rims around nodules, and the truncation of aragonitic fossils (ammonoids).

#### 6.1.1. Fractures in the nodules

Some fractures observed within the nodules do not extend into surrounding matrix suggesting that the nodules had already been lithified before mechanical compaction began. Similar observations were made by Bosellini and Ferri (1980) in a section of the same formation in the central Dolomites. The fractures are filled by calcite or chalcedony, micrite or by the surrounding sediment. A polyphase infill is often observed, whereby the earliest infill is either micrite or calcite cement (Fig. 5A,B). Fractures with sharp boundaries and blocky calcite infilling, attributed to deep burial or Alpine deformation, cross cut the nodules, the surrounding sediments and the early fractures (Fig. 5).

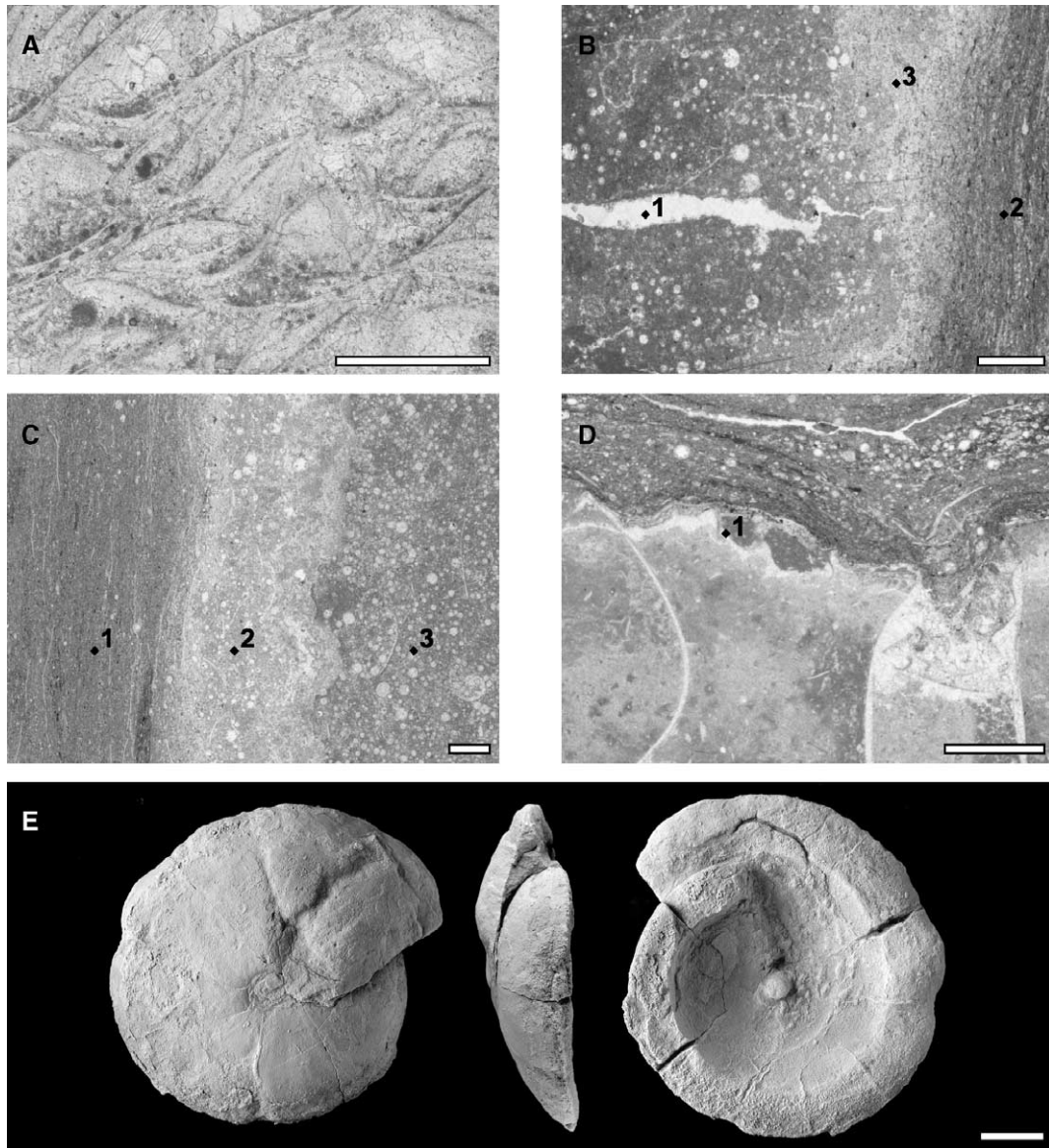


Fig. 5. Evidence of early lithification and dissolution in the Knollenkalke Mb., Rio Sacuz section. Thin-section photomicrographs were taken in plain-polarized light, scale bars 1 mm except (E). See text for further explanation. (A) Uncompacted bivalve coquina. (B) Brittle fracture (1) in a nodule that does not continue into the embedding matrix (2). Note silicification front (3) at the nodule–matrix boundary. (C) Silicification front (2) between a nodule (1) and the surrounding matrix (3). (D) Dissolution surface (1) on the upper side of an ammonoid shell. (E) Partly dissolved ammonoid (arcestid). This group of ammonoids had subspherical shells and at least 3/4 of the shell was dissolved in this specimen. Sample whitened using magnesium oxide, scale bar 1 cm.

#### 6.1.2. Reworking of nodules

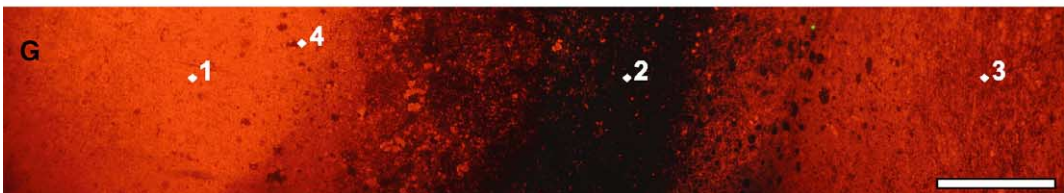
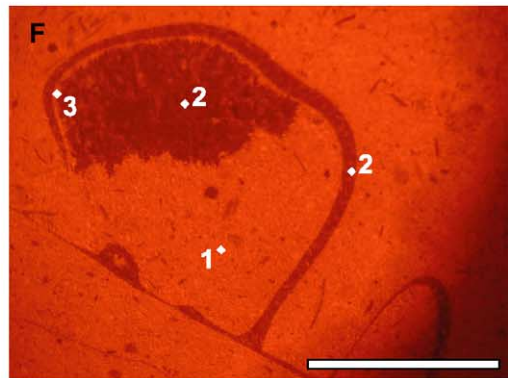
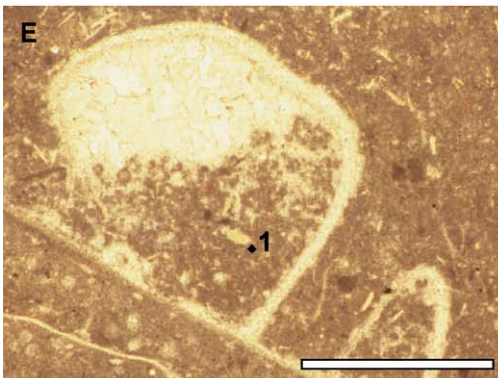
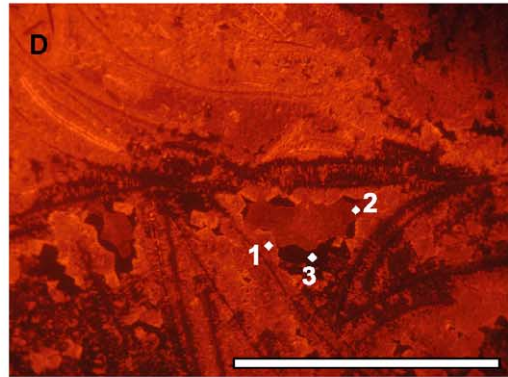
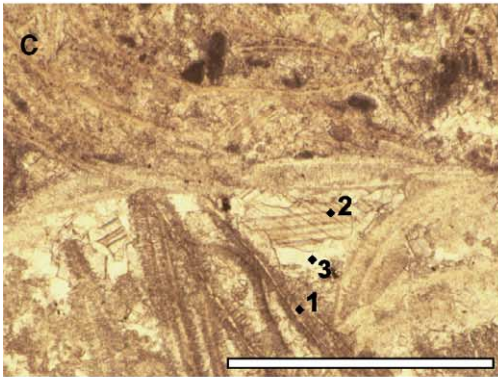
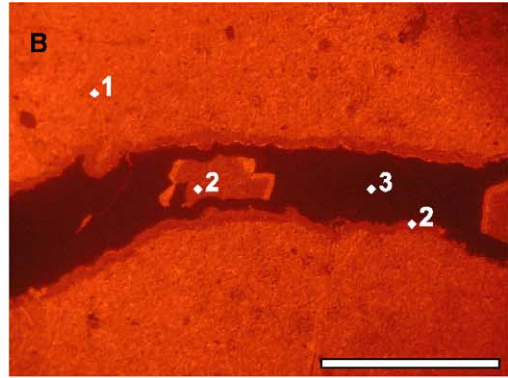
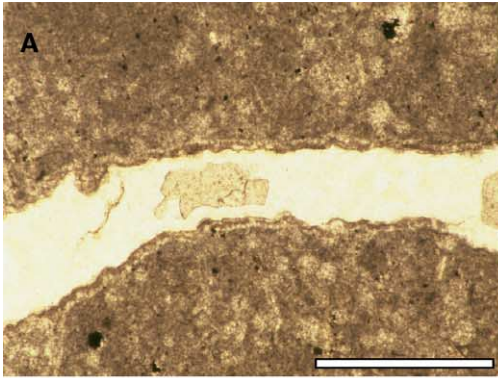
At Rio Sacuz, slumps involving the uppermost 10–20 cm of sediment are observed. Two types of slumps were identified, whose detachments are always bound to thin ash layers. The first type of slumps gave rise to

plastic deformation in the Knollenkalke. This deformation is locally accompanied by water-expulsion structures, indicating hydroplaning of the slump. The second type of slumps produced a brittle deformation of the sediments involved, which show small-

scale fractures along the axes of the slump folds testifying partial lithification of the beds.

Accumulations of nodules are locally associated with both kinds of slumps, including those that

involved only a few centimetres of sediment. These deposits imply that nodules began to form within a few centimetres beneath the sediment surface and are not a result of burial diagenesis. Similar reworked



nodules were also described by Bosellini and Ferri (1980).

### 6.1.3. Uncompacted coquinas

Thin-shelled bivalve coquinas, observed at Rio Sacuz, are bivalve grainstones, interpreted as turbidites (cf. Maurer et al., 2003). Such sediments are expected to undergo strong compaction during shallow burial (e.g., Clari and Martire, 1996). The coquinas of Rio Sacuz instead show little evidence of compaction and exhibit wide open pore spaces between bivalve shells filled by at least three generations of cement (Figs. 5A; 6C,D). The earliest cements are syntaxial calcitic overgrowths on bivalve shells. This cement appears to have lithified the coquina framework prior to shallow burial and is probably also responsible for the early lithification of the nodules. Chalcedony and a later generation of calcite cements grew above the syntaxial cements. Coquinas with similar characteristics were found in the pelagic condensed facies draping the slopes of the Cernera platform in various localities (e.g., Piz del Corvo).

### 6.1.4. Silicified rims around nodules

Most nodules are outlined by a silicified rim, whose thickness is on the order of few millimetres. The silica content is higher near the outer part of the nodule and decreases rapidly toward the inner part (Figs. 5B,C; 6G). Inside the nodule, silica — generally in the form of chalcedony — fills a few of the larger voids (e.g., radiolarian moulds) or penetrates along bioturbation traces. Thin-section petrography suggests that the replacement of calcite by chalcedony progressed relatively easily throughout the nodule matrix, but did not reach the interior of the nodules. Early lithification of the nodules by early calcite cement resulting in a significant permeability reduc-

tion probably prevented diffusion of silica-rich fluids into the interior of the nodules.

### 6.1.5. Ammonoid truncation

Ammonoids are the only aragonitic macrofossils found in the Knollenkalke. Despite the pelagic setting, these fossils are surprisingly uncommon. Ammonoid-bearing horizons in the Knollenkalke were found at Rio Sacuz, San Marco and Bagolino. In all these sites the upper part of ammonoid shells (typically, 50% to 90% of the shell) is truncated. The lower face of the shells is consistently better preserved than the upper one (Figs. 5E, 7F). These truncated shells are typically replaced by sediment from the overlying bed. As this truncation is restricted to the upper shell surface only, pressure solution can be ruled out. These features therefore demonstrate that the aragonite of the shells underwent dissolution already at the water–sediment interface and that the micritic infill of the ammonoid was partially lithified prior to burial.

### 6.2. Origin of a single turbidite bed, San Marco section

Sam 36 is a ca. 15 cm-thick, reddish bed in the lowermost part of the Knollenkalke Mb. below marker bed Tc in the San Marco section that is particularly instructive for the issue of aragonite dissolution. It is constituted by a packstone with shallow and deep-water bioclasts (Fig. 7B). Many bioclasts, and particularly almost all shallow-water fossils, are associated with a reddish-brown micrite that locally gives rise to geopetal structures. Many geopetal infills are turned upside down (Fig. 7C) demonstrating that bioclasts were at least partially cemented before their reworking into bed Sam 36. At the regional scale, the only coeval sediments showing similar characteristics are the Ladinian “Ammonitico Rosso” (Clapsavon Limesto-

Fig. 6. Calcite cements in transmitted light and CL, scale bars 1 mm. (A) Early diagenetic fracture in a nodule with polyphase filling, Knollenkalke Mb., Rio Sacuz. (B) Same sample as in (A), under CL. The bulk of the nodule appears bright luminescent (1), while the later fracture-fill calcite (2) is slightly less luminescent and partly zoned. The remainder of the fracture is filled by non-luminescent chalcedony (3). (C) Bivalve coquina showing early calcite overgrowth (1) and a few large cavities filled by chalcedony (3) and sparry calcite of a later generation (2), Knollenkalke Mb., Rio Sacuz. (D) Same as (C), under CL. The early calcite overgrowths (1) are bright luminescent, while late-stage calcite (2) associated with chalcedony (3) is dull luminescent. (E) Shelter cavity with geopetal infill of micrite peloids (1) within an ammonoid shell, Knollenkalke Mb., Rio Sacuz. (F) Same as (E), under CL. Micrite peloids and their early cement coatings appear both bright luminescent (1), while the ammonoid shell and the late calcite cement filling the upper part of the shelter cavity appear weakly luminescent (2). Note the fringe of bright luminescent early calcite cement (3) in the upper part of the cavity, which apparently coated the ammonoid shell prior to its dissolution and substitution by calcite. (G) Photomosaic showing the boundary of a nodule under CL, upper transitional interval, Rio Sacuz. From left to right: bright luminescent nodule (1), non-luminescent silicification front (2), dull luminescent matrix (3). Some radiolarian moulds (4) are filled by dull luminescent calcite.

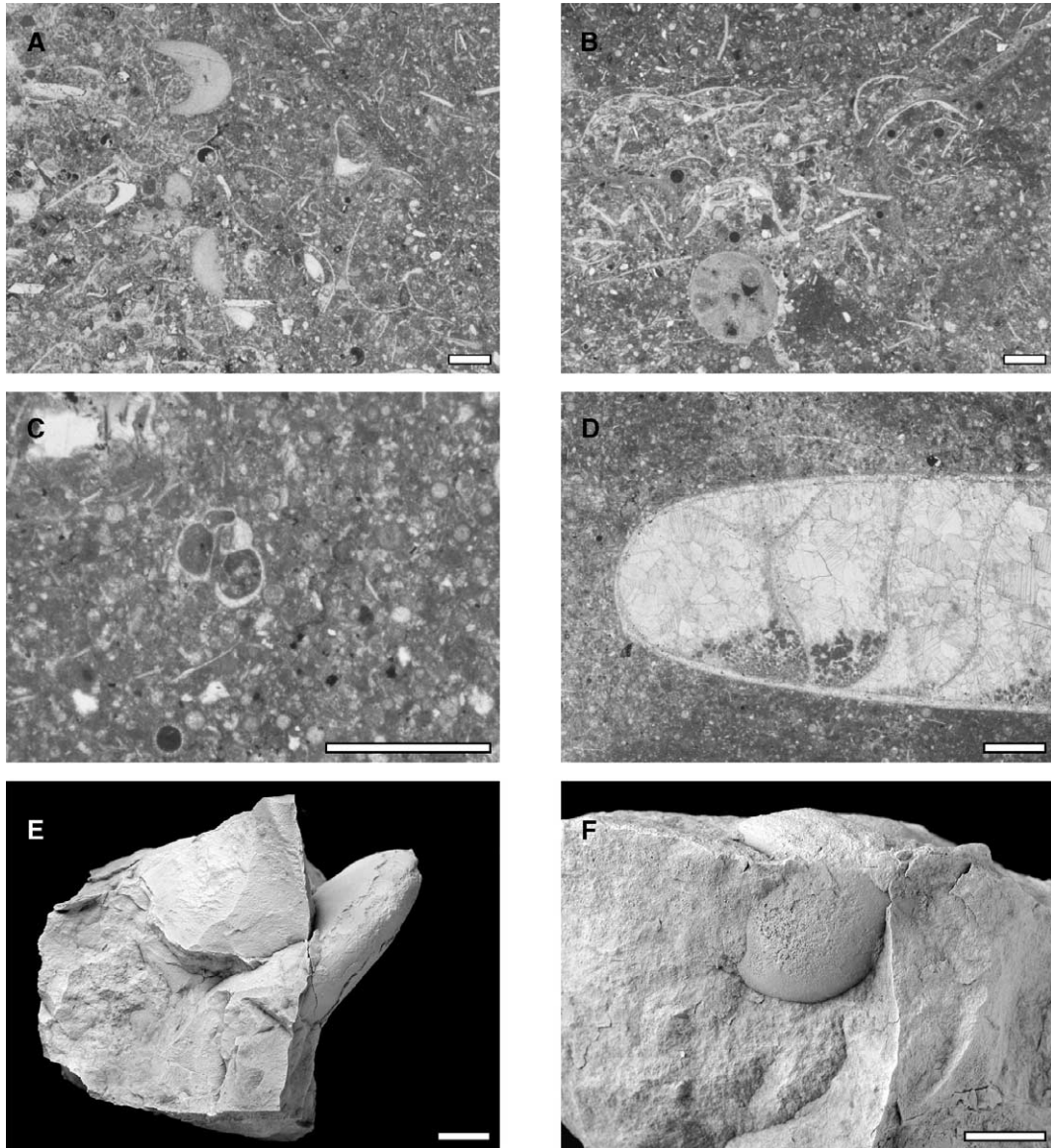


Fig. 7. Characteristics of bed Sam36. Thin-section photomicrographs were taken in plain-polarized light, scale bars 1 mm. (A) Thin section of the Clapsavon limestone (so-called Ladinian Ammonitico Rosso), deposited on top of drowned platforms of Carnia. (B) Thin section of bed Sam36. (A) and (B) illustrate the similarities between bed Sam36 and the coeval platform drowning facies. (C) Geopetal infill in a gastropod shell. The oblique or vertical position of these geopetals demonstrates later reworking. (D) Well preserved ammonoid shell with non-reversed geopetal infill. (E) Ammonoid (*Parasturia emmrichi*) from the lower part of the bed, deposited in oblique position. (F) Ammonoid (Arcestitid) truncated by dissolution at the top of the bed. Hand specimens were whitened using magnesium oxide, scale bars 1 cm.

ne=Calcare del Clapsavon, e.g., Casati et al., 1982) capping drowned carbonate platforms in the eastern Dolomites and Carnia (Fig. 7A). Apart from normal grading and vertical escape traces, no sedimentary structures were recognizable in bed SAM 36. The

base of the bed is irregular; the top is flat and is overlain by a few centimetres of red clay.

We interpret bed Sam 36 as resulting from a single turbidity current largely composed of reworked sediments from the top of a drowned carbonate platform.

Incidentally, bed Sam 36 at San Marco provides a minimum age for the drowning of this carbonate platform, which was most probably located at the nearby Cadini Mountain.

Ammonoid shells, the only elements reaching centimetre dimensions in this bed, are randomly oriented (Fig. 7E). Ammonoids at the top are truncated and their tests are replaced by micritic sediment (Fig. 7F). In contrast, ammonoids in the lower part of the bed show well preserved shells diagenetically replaced by calcite (Figs. 7D,E). Truncation and dissolution occurred only after the deposition of the turbidite at the sea bottom. The substitution of the tests by micritic sediments suggests dissolution of aragonite and lithification of the embedding sediment prior to burial, i.e., near the water–sediment interface.

### 6.3. Cementation history of the Knollenkalke

Optical, CL and SEM observations allow to recognize multiple phases of cementation by calcite and chalcedony.

#### 6.3.1. Bright luminescent syntaxial calcite

The earliest cements are syntaxial calcite overgrowths on echinoderms and thin-shelled bivalves, which are particularly common in bivalve coquinas. This cement appears pale brown in transmitted light, and shows uniformly bright orange CL. Rare remains of formerly aragonitic fossils (mostly ammonoids) are also surrounded by a fringe of pale brown luminescent calcite cement (Fig. 6F). Syntaxial overgrowths on thin-shelled bivalves observed under the SEM appear as carpets of crystals with rhombohedral ter-

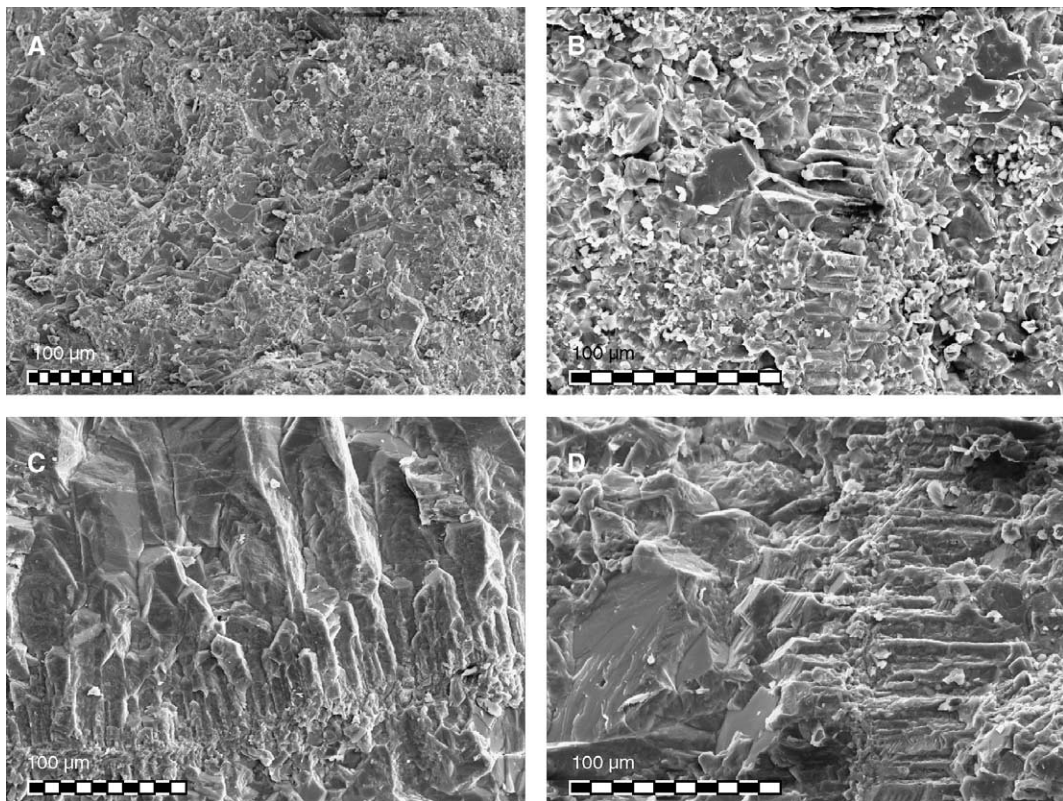


Fig. 8. SEM images of Knollenkalke samples. (A) Sediment surrounding nodules is composed of blocky calcite cement; the material constituting the rest of the sample is silica cement. (B) Thin-shelled bivalve in a nodule showing a syntaxial overgrowth. Most of the sediment is micrite; radiolarian moulds are filled by blocky calcite. (C) Syntaxial overgrowth on a thin-shelled bivalve; crystals show the typical rhombohedral terminations of calcite. (D) Syntaxial overgrowth on a thin-shelled bivalve, with rhombohedral terminations; in the left part of the picture, a large pore is filled by blocky calcite.

minations, confirming that these early cements formed as calcite (Fig. 8A).

### 6.3.2. Dull luminescent calcite and chalcedony

A later generation of cement (Fig. 8B) appears as inclusion-poor blocky calcite. This calcite is weakly luminescent when viewed under CL illumination. CL-zonation was observed in larger crystals. Both zoned and dull luminescent calcite cements are associated with chalcedony in bivalve coquinas, in fractured nodules and within the matrix of nodules. As calcite grew both before and after chalcedony (Fig. 6A,B), dull luminescent calcite and chalcedony precipitated almost contemporaneously. Calcite fills primary voids in bivalve coquinas postdating precipitation of fringes of the first generation calcite (Fig. 6C,D), early fractures in nodules that do not continue into the surrounding sediments (Fig. 6A,B), and radiolarian moulds within some nodules, in particular those near the margins of the nodules (Fig. 6G). Calcite also replaced aragonitic shells (Fig. 6E,F). This implies that the zoned and dull luminescent calcite precipitated only after the onset of compaction, i.e., related to burial diagenesis.

### 6.3.3. Late-stage calcite in fractures

The last generation of fractures cross-cutting both nodules, the surrounding sediment and earlier fractures, probably originated during deep burial and/or Alpine deformation. These late-stage fractures are filled by blocky calcite that appears very bright orange-yellow under CL. The volume represented by this third generation of calcite, however, is negligible.

### 6.3.4. Distribution of cements as a function of the lithology

The bright luminescent, syntaxial calcite was responsible for the early lithification of nodules and bivalve coquinas, while the nodule matrix is lithified by dull luminescent calcite and chalcedony. Indeed, nodules appear brighter under CL than matrix calcite (Fig. 6G). Micrite inside nodules shows the same CL colour as bright syntaxial calcite. This micrite, derived from surrounding carbonate platforms, was probably aragonitic in composition (Stanley and Hardie, 1998), but is now replaced by

bright luminescent, syntaxial calcite. Munnecke et al. (1997) illustrate calcite microspar substituting aragonite mud in both recent (Upper Pliocene of Bahamas) and ancient (Silurian of Gotland) shallow burial environments. The bright luminescent calcite of Knollenkalke nodules, however, is remarkably different from that of Munnecke et al., in being true micrite (most crystals are  $<4\ \mu\text{m}$ ) and because of the absence of residual aragonite needles or pits. The nodules are thus principally composed of bright luminescent syntaxial calcite, plus some calcitic bivalves, dull luminescent calcite-filled large pores, and late-stage calcite in fractures. Some bivalve coquinas of the Rio Sacuz section are also composed by brightly luminescent, syntaxial calcite and calcitic bivalves, with dull luminescent calcite and micrite as minor components (Figs. 5A, 6C,D). The lithification of the nodules and bivalve coquinas by bright luminescent syntaxial calcite predated mechanical compaction. On the contrary, calcite of the nodule matrix is dull luminescent. Platform-derived micrite is largely absent in this matrix. Dull luminescent calcite and chalcedony lithified the matrix after the onset of compaction (Fig. 5B–D).

### 6.4. Stable isotopes

The carbon and oxygen isotope composition of 74 samples from the Plattenkalke–Knollenkalke transition and from the Knollenkalke Mb. of Rio Sacuz, and 56 samples from the Knollenkalke Mb. of Palus–San Marco was analyzed. The isotope composition of nodules, matrix and calcite veins from Rio Sacuz plot in three distinct fields (Fig. 9A). The isotope composition of bivalve coquinas is similar to that of the nodules. The composition of coquinas and nodules ( $\delta^{13}\text{C}=0.8\pm 0.5\text{‰}$ ,  $\delta^{18}\text{O}=-3.3\pm 0.8\text{‰}$ ) is within that of Triassic seawater, as determined from calcitic brachiopods (Veizer et al., 1999). Matrix and late-stage vein calcite show depleted oxygen isotope values. The samples from Palus–San Marco show a somewhat different picture (Fig. 9B). The average carbon isotope composition of all petrographic constituents is similar, but the oxygen isotope values are more negative than in the Rio Sacuz section (e.g., nodules:  $\delta^{13}\text{C}=0.9\pm 0.3\text{‰}$ ,  $\delta^{18}\text{O}=-5.7\pm 1.5\text{‰}$ ), and the isotopic compositions of nodules, matrix and late

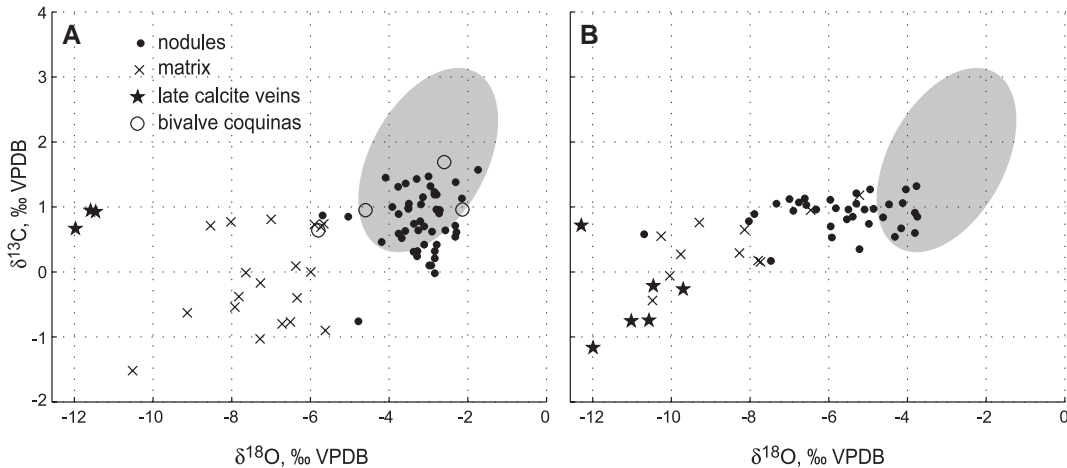


Fig. 9. Carbon and oxygen isotopic composition of nodules, bivalve coquinas, matrix of nodules and late diagenetic calcite veins in the Knollenkalke Mb. The average isotope composition of Triassic seawater based on data from brachiopod shells (Veizer et al., 1999; average compositions  $\delta^{13}\text{C}=1.7 \pm 1.2\text{‰}$  and  $\delta^{18}\text{O}=-3.0 \pm 1.5\text{‰}$ , including the error ellipse of the bivariate normal distribution) is shown by the grey fields. (A) Rio Sacuz: the three main categories, i.e., nodules, matrix and calcite veins, plot in three distinct fields, while the isotopic composition of bivalve coquinas show similar compositions as the nodules. (B) At San Marco, both the nodules and matrix calcite are shifted toward lower O isotope values suggesting a stronger diagenetic impact than at Rio Sacuz.

calcite veins partly overlap. We suggest that these isotopic differences between the two sections are the result of a more intensive burial diagenetic overprint of the Palus–San Marco section. Conodonts from the latter locality yielded a Colour Alteration Index (CAI) of 1.5 to 2, corresponding to a maximum burial temperature of 90–140 °C (Epstein et al., 1977), while the CAI of conodonts at Rio Sacuz is 1, corresponding to 50–80 °C.

In both sections carbon and oxygen isotope values of matrix samples are correlated, in contrast to the nodules, whose isotope values do not covary (Table 3).

Because of the generally lower diagenetic overprint the Rio Sacuz section was selected for a study of stable isotope variations through time. (Fig.

10A,B). Oxygen isotope values remain constant throughout the section, and matrix samples are consistently depleted with respect to nodules. The  $\delta^{13}\text{C}$  values of nodules show an increase of ca. 1.5‰ along the 29 m long section. Matrix samples in the transitional interval are distinctly depleted in  $^{13}\text{C}$ , and evolve toward a composition similar to that of the Knollenkalke.

## 7. Discussion

### 7.1. Sedimentation rates vary in time and space

Triassic deep-water carbonates are widely considered as formed at rather constant sedimentation rates. This appears particularly true for the Plattenkalke, which contain little sediment derived from carbonate platforms (e.g., Maurer and Schlager, 2003; Maurer et al., 2003). Our study, however, supports previous reports in favour of significant variations in sedimentation rate (Muttoni et al., 2001; Channell et al., 2003) in similar deep-water (up to 1000 m deep), hemipelagic settings (Tables 1 and 2).

The four basinal sections considered here belong to two groups: sections containing Plattenkalke (Rio Sacuz and Seceda), and sections where the Platten-

Table 3  
Correlation coefficients between  $\delta^{13}\text{C}$  and  $\delta^{18}\text{O}$  from Rio Sacuz and Palus–San Marco sections, calculated separately for nodules and matrix

Lithology\Section	Rio Sacuz	Palus–San Marco
Nodules	<i>0.16</i> (n=48)	<i>0.20</i> (n=35)
Matrix	0.54 (n=21)	0.71 (n=15)

Correlation coefficients are significant at the 95% level for matrix, while are not significantly different from zero in nodules (italic).

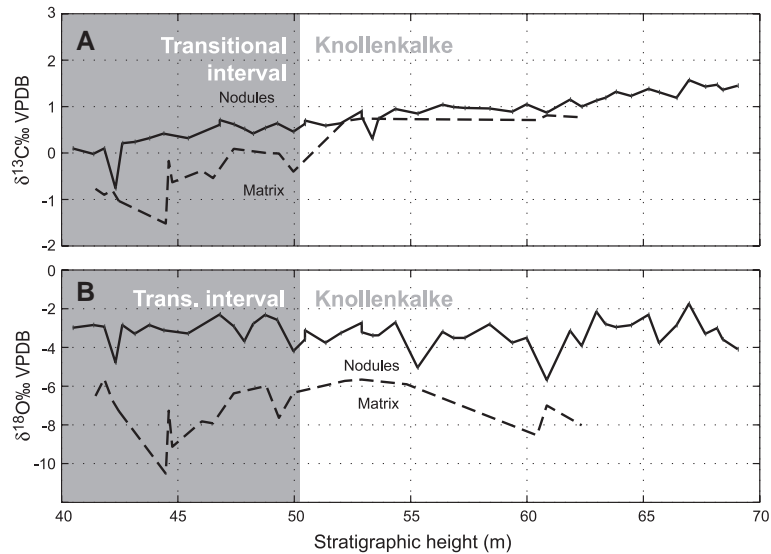


Fig. 10. Carbon and oxygen isotopes in the transitional interval (in grey) and the Knollenkalke Mb. at Rio Sacuz. The oxygen isotope composition of nodules is always higher than that of the surrounding sediment reflecting differential diagenesis. Carbon isotopes of the nodules show only limited short-term variations and a long term increase of 1.5‰. Lower carbon isotopes in the matrix of the transitional interval reflect a relatively high organic carbon content.

kalke are substituted by an oxygenated facies, more similar to the Knollenkalke (San Marco and Bago-lino). We assume that sedimentation rates are more constant in sections of the second group where facies variations are small. As the Plattenkalke are always thicker than their correlative intervals in sections of the second group, it appears that the sedimentation rate of the Plattenkalke was high with respect of that of the Knollenkalke (or of similar well-oxygenated facies).

A further indication of this is given by the ca. 9 m-thick marl–limestone stack occurring between Plattenkalke and Knollenkalke at Rio Sacuz. Such couplets may be generated by environmental oscillations forced by orbital parameters, or by an unidentified sedimentary process; either way, it can be assumed that each couplet represents in average a constant amount of time. Under this assumption, the upward decrease in thickness of the couplets indicates an upward decrease in sedimentation rate.

The interpretation of the Plattenkalke as the pelagic facies forming in absence of sediment supply from carbonate platforms (Maurer and Schlager, 2003; Maurer et al., 2003) implies that sedimentation rates of the Plattenkalke were lowest within the Livinallongo Fm., and that during the deposition of

the Plattenkalke carbonate platforms were not (yet) productive.

Both points are inconsistent with the results of this study, as (1) the Plattenkalke, where present, always show a greater thickness than correlative, oxygenated facies in other sections, and (2) the  $\geq 180$  m-thick portion of the Latemar platform with *A. avisianum* is correlated with the lower–middle part of the Plattenkalke, and perhaps with the uppermost part of the underlying Ambata Fm. (Fig. 4). *A. avisianum* also occurs at Punta Zonia below the layers documenting the drowning of the Cernera platform (Fig. 3). Thus, the Latemar as well as the Cernera carbonate platforms were productive during deposition of the Plattenkalke.

Following Maurer and Schlager (2003), only a minor part of the micrite in the Knollenkalke could possibly be ascribed to “pelagic rain”, while most of the carbonate was derived from surrounding carbonate platforms, not necessarily as recognizable calcareous turbidites. The Plattenkalke were regarded as “background sedimentation” because of the scarcity of calcareous turbidites and because of the persistence of bedding patterns on a km-scale (Maurer and Schlager, 2003). Both these characteristics, however, can also occur in a basin partially fed by platform carbo-

nate, if organic matter availability results in the dissolution of carbonates (i.e., not only aragonitic shells, but all carbonate grains).

Finally, carbonate platforms are not generally expected to provide a constant supply of micrite to the basins. For example, large variations of sedimentation rates were found in most analyses of the coeval Latemar platform interior (Goldhammer et al., 1987; Preto et al., 2001; Zühlke et al., 2003).

## 7.2. Deep-water aragonite dissolution as a factor influencing sedimentation

### 7.2.1. Mechanism of aragonite dissolution

The main process leading to carbonate dissolution above the calcite (or aragonite) compensation depth is the enhanced acidity of pore waters due to microbial decomposition of organic matter during the very shallow burial (Munnecke et al., 1997; Cherns and Wright, 2000; Wright et al., 2003; and references therein). This was also, most likely, the main dissolution process during the deposition of the Plattenkalke and Knollenkalke. Aragonite dissolution and reprecipitation as calcite must have occurred very early during shallow burial of the Knollenkalke, in order to explain the observed features of early lithification.

Despite the growth of healthy carbonate platforms during the deposition of the Plattenkalke, its major constituents are silica and organic carbon; carbonates (mostly dolomite at Rio Sacuz) constitutes less than 30% of the bulk sediment. The low carbonate content might be explained by the availability of larger amounts of organic matter and, thus, higher pore water acidity. Carbonate fossils are in fact very rare in the Plattenkalke, except when early lithification allowed their preservation (Maurer and Schlager, 2003). Since the carbonate-depleted Plattenkalke exhibit the highest sedimentation rates of the otherwise carbonate-rich Lower Livinallongo Fm., it must be assumed that sediment shedding from coeval carbonate platforms cannot be the sole control on sedimentation rate variations of Middle Triassic hemipelagites of the Southern Alps. The same holds for carbonate dissolution.

### 7.2.2. Dissolution and omission surfaces

The nodular appearance of the Knollenkalke Mb. closely resembles that of the Jurassic Ammonitico

Rosso; this similarity extends well beyond the nodular structure, and involves all the aforementioned early diagenetic features of the Knollenkalke. The Ammonitico Rosso is well known for the evidence of early dissolution of aragonite shells (e.g., Schlager, 1974), very early cementation that gave rise to its conspicuous nodular structure (Clari and Martire, 1996), and abundant condensation and omission surfaces.

Evidence for small hiatuses within the Knollenkalke Mb. is provided by magnetostratigraphic correlation with the sections at Seceda and Frötschbach (Muttoni et al., 2004). Two minor discrepancies are observed between these sections: (1) a switch from reverse to normal polarity is present in the Seceda core exactly at the Plattenkalke–Knollenkalke boundary, while at Frötschbach this switch is not present. A short reversal including Tc (F1n.1r) is present at Frötschbach, which was not found at Seceda despite very narrow sampling. Minor omission surfaces at Seceda may account for these discrepancies. An omission surface at the base of the Knollenkalke can also explain the sharp boundary between Plattenkalke and Knollenkalke of Seceda (Brack and Muttoni, 2000), coincident with the polarity switch, not observed in other localities.

### 7.2.3. Biostratigraphic bias

The ammonoid assemblages recovered in the Southern Alps from the Knollenkalke (Brack and Rieber, 1986; 1993; Brack et al., 2003; Mietto et al., 2003a) appear biased by dissolution processes. Ammonoid assemblages are of great importance, because the Triassic biostratigraphy relies primarily on ammonoids, and a widely used ammonoid biostratigraphic scale for this time interval was developed in Knollenkalke successions (Brack and Rieber, 1993).

Given the fact that all ammonoid specimens from the Knollenkalke show evidence of partial dissolution, it is likely that many other ammonoid shells were originally present at the water–sediment interface, but were completely dissolved prior to burial. Small ammonoids and ammonoids with thin shells are the most likely candidates for complete dissolution, giving rise to an incomplete and biased ammonoid assemblage of the Knollenkalke Mb. Two sets of observations support this model.

Firstly, the ammonoids of the Knollenkalke Mb. are always relatively large (>4 cm); none of our ammonoid specimens is a juvenile form, neither have juveniles been illustrated in previous studies. Secondly, ammonoid associations in storm layers of the coeval platforms, including the Latemar (Mojšisovics, 1882; Brack and Rieber, 1993; De Zanche et al., 1995; Manfrin et al., 2005), are distinctly different, and include, among large individuals, small taxa (*Aplococeras* spp., *Lecanites* sp., *Celtites* spp.) and many juveniles, which are practically absent in the Knollenkalke. It might be argued that small taxa were confined to peri-platform areas, and are therefore absent in the Knollenkalke (e.g., Brack and Rieber, 1993). We reject this explanation, however, because it cannot account for the absence of juveniles in the Knollenkalke, and because representatives of the small genus *Aplococeras* are common in the marls and shales of the basinal Ambata Fm. and correlative units (Fig. 4; cf. also Mietto et al., 2003a,b; Manfrin et al., 2005). In our view, the only explanation for the absence of small ammonoid taxa and juveniles in the Knollenkalke is that they were dissolved at the water–sediment interface. This implies that a reliable documentation of Middle Triassic ammonoid assemblages from the Knollenkalke is impossible.

Preferential dissolution of aragonite shells (so-called “taphonomic loss”) has been documented in the Silurian (Cherns and Wright, 2000) and in the Lower Jurassic (Wright et al., 2003). The biostratigraphic bias present in the Knollenkalke therefore supports reports that Paleozoic and Mesozoic pelagic fossil assemblages may be severely biased by dissolution.

### 7.3. Deep-water dissolution, carbonate platform drowning and ocean water circulation in the western Tethys

#### 7.3.1. Seawater during deposition of the Knollenkalke

In part of the Dolomites, the change from the Plattenkalke to the Knollenkalke documents a switch from anoxic–dysoxic to well-oxygenated bottom waters and is thus related to a change of the ocean circulation at a regional scale (Brack and Muttoni, 2000). Anoxic–dysoxic conditions at the sea floor are documented by the preservation of organic matter and the presence of pyrite and lamination in the

Plattenkalke. Outside the depositional area of the Plattenkalke, however, sedimentation of the Knollenkalke began roughly at the same time: at San Marco, the base of the Crassus Subzone is located ca 4 m below the base of the first nodular limestones, and at Bagolino, while the deposition of nodular limestones already began during the Avisianum Subzone, a nodular-cherty facies also started above the base of the Crassus Subzone (Mietto et al., 2003a; Fig. 1). Within the biostratigraphic resolution the base of the Knollenkalke is thus coeval in large parts of the Southern Alps.

Contemporaneous dissolution of aragonite shells and deposition of calcite demonstrate that the bottom water during the deposition of the Knollenkalke was undersaturated with respect to aragonite, but supersaturated with respect to calcite. Assuming a Mg/Ca ratio of ca. 3 for Triassic seawater (Stanley and Hardie, 1998), the temperature must have been lower than 10–15 °C in order to precipitate calcite (Morse et al., 1997). The characteristic nodular structure of the Knollenkalke, requiring contemporaneous aragonite dissolution and calcite precipitation to form, is a consequence of the saturation state of bottom water, as determined by its temperature. Thus, the base of the Knollenkalke Mb. is not a simple lithological boundary but probably marks the arrival of a cool water mass in the Southern Alps. We suggest that a progressive increase of basin interconnectivity during Crassus–Chiesense times, coupled with strong subsidence and exceptionally high sea level (Gianolla and Jacquin, 1998), led to the inflow of cool deep ocean waters from Panthalassa into the western Tethys.

The onset of the Knollenkalke facies at Felsöors (Balaton Highlands, Hungary) also dates to the Chiesense Subzone (Vörös et al., 1996). At the same time, nodular cherty limestones were forming also in the Northern Calcareous Alps (Reifling Lms.).

#### 7.3.2. Carbonate platform drowning in the Southern Alps

Several carbonate drowning events occurred between the Early Anisian and the Early Ladinian in the Dolomites: the Anisian Contrin carbonate bank drowned in several localities, including Seceda; some carbonate platforms interfingering with the Livinalongo Fm. were also subject to the same fate, but the timing of their drowning is not always well con-

strained. On the contrary, the time of drowning of the platforms adjacent to the basal sections considered here is fairly well known.

The Cernera platform, adjacent to Rio Sacuz and Punta Zonia, drowned during the Crassus Subzone. This is documented by the onset of condensed hemipelagic limestones above distal slope grainstones in the Punta Zonia section. At the same time, the change to the Knollenkalke facies and a drop of the sedimentation rates occurred at Rio Sacuz on the opposite side of the platform.

The Cadini platform, adjacent to San Marco, was also (partially?) drowned at the time of deposition of bed SAM 36, within the Crassus Subzone, as bed SAM 36 contains reworked material from this drowned platform.

The Latemar and Marmolada platforms survived the event that led to the drowning of Cernera as demonstrated by the occurrence of ammonoids of the Secedensis Subzone (Manfrin et al., 2005). Nevertheless, the Marmolada platform must have also experienced partial drowning, as red pelagic limestones seal the slope of this platform at Col Mer and La Grea, and yielded ammonoids of the Crassus Subzone (Blendinger, 1994; De Zanche et al., 1995). More generally speaking, carbonate platforms of the western Dolomites seem to have survived this drowning event, while platforms of the central-eastern Dolomites often drowned (Fig. 2). The onset of a new circulation pattern in the Southern Alps, however, appears synchronous with the carbonate platform drowning event.

It was suggested that the Cernera platform was a topographic threshold and the eastern boundary of a restricted basin where the Plattenkalke were deposited. After the drowning of Cernera, a seaway opened and this new ocean circulation pattern eventually triggered the deposition of the Knollenkalke (Brack and Muttoni, 2000). Although intriguing, this explanation is rejected, because the Plattenkalke occur also east of Cernera (e.g., Ru Sec, De Zanche et al., 1995). In addition, Rio Sacuz is located on the south-eastern flank of Cernera, also outside the hypothesized restricted basin.

### 7.3.3. Late Anisian–Early Ladinian upwelling in the western Tethys ocean?

As discussed above the inflow of bottom waters causing aragonite dissolution in the Dolomites took

place within a few ammonoid biochronozones. During the Late Anisian to Early Ladinian strong monsoonal conditions prevailed in the Tethys region (Kutzbach and Gallimore, 1989). The opening of a seaway in the east resulted in the inflow of bottom waters into this gulf. Strong seasonal trade winds related to the monsoonal climate caused coastal upwelling in this sector of the western Tethys. Upwelling water is relatively cool and rich in inorganic carbon, because it dissolved aragonite at the sea floor just before reaching the surface. This scenario can explain several aspects of the Uppermost Anisian to Lower Ladinian evolution of the Southern Alps and of other parts of Europe.

Firstly, the continental-scale distribution of the Knollenkalke facies, which is in sharp contrast to the complex pre-Knollenkalke stratigraphy, is in agreement with increased basin interconnectivity. Secondly, inflow of cool bottom waters can account for the onset of aragonite dissolution at the sea floor; relatively low temperatures are also required for the observed precipitation of calcite. Thirdly, upwelling of cool waters can also explain the drowning of some platforms during Crassus–Chiesense times. Carbonate production of platforms in upwelling areas could have been slowed down by the drop in water temperatures. Carbonate platforms that drowned during this time are located in the eastern Southern Alps (i.e., closer to the connection with Panthalassa), while all platforms of the western Dolomites survived at least through the Crassus Subzone (Fig. 2). Crises of platform carbonate production due to cool water have been demonstrated for modern carbonates (e.g., Roberts et al., 1982), although on a much shorter time scale. The mud-mound nature of the surviving Ladinian carbonate platforms (e.g., Blendinger et al., 2004) may also be a consequence of this upwelling, as suggested for Carboniferous carbonate mud-mounds (Wright, 1994).

### 7.4. Carbon isotopes as a proxy for the carbon isotopic composition of seawater

The remarkable differences in carbon and oxygen isotopic composition of nodules, matrix and secondary calcite veins are explained by the distribution of different generations of cements in these sediment components. Cement of nodules is mostly bright luminescent syntaxial calcite. Micrite, the dominant component of nodules, most likely formed as aragonite but

was replaced by calcite showing the same CL characteristics as the early syntaxial cement. The matrix surrounding nodules is mostly composed of dull luminescent calcite and chalcedony, while late-stage calcite precipitated in fractures.

The isotope composition of nodules, composed of very early diagenetic calcite, is used as a proxy for the isotope composition of bottom seawater. This is supported by four lines of observations: (a) O isotope values become progressively lighter from nodules to matrix to late-stage vein calcite (Fig. 9), consistent with the expected diagenetic pathway (i.e., the isotopic composition of the nodules is closest to the initial composition). (b) C and O isotope values of nodules are uncorrelated, but they are significantly correlated in matrix samples (Table 3), again suggesting a higher degree of diagenesis in the latter. (c) The isotope compositions of bivalve coquinas of Rio Sacuz, composed mostly of very early diagenetic, syntaxial calcite, plot in the same field as the nodules (Fig. 9A). (d) The isotopic composition of the nodules overlaps that of carbonate precipitated from Triassic seawater (Fig. 9).

We therefore regard the C isotope composition of the nodules as a reliable proxy of the C isotopic composition of the former bottom water. The carbon isotopic compositions of nodules of the same stratigraphic intervals at Rio Sacuz and Palus–San Marco are identical, while the O isotope values differ by more than 2‰, attributed to diagenesis at higher burial temperatures at Palus–San Marco (consistent with CAI data). More generally speaking, while the O isotope values of the Knollenkalke are altered by diagenetic processes, the C isotope values appear pristine and their long-term evolution is briefly discussed for the Rio Sacuz section, where the  $\delta^{13}\text{C}$  increases by 1.5‰ through a 29 m section. More data from other sections are required to determine the origin of this isotope excursion in the Lower Knollenkalke, and two hypotheses are briefly offered here. The  $\delta^{13}\text{C}$  increase might reflect increasing inflow of bottom water from Panthalassa, if these waters had a relatively high carbon isotope ratio. This scenario is in agreement with the observed upward increase of dissolution features in the Rio Sacuz section. Alternatively, the increase in  $\delta^{13}\text{C}$  might reflect progressive burial of light organic C on a regional scale. This second scenario is consistent

with the observation that black shales and organic carbon-rich basinal limestones are widespread in the Southern Alps, but decrease in abundance throughout the studied interval.

## 8. Conclusions

High-resolution correlation between the Middle Triassic deep-water Ambata and Livinallongo Formations of the Dolomites are extended to the Latemar carbonate platform section. Correlations show that (a) hemipelagic sedimentation rates varied by up to a factor of 10, with the lowest sedimentation rates in the GSSP of the base Ladinian (Bagolino, Lombardian Alps), and (b) the Plattenkalke Mb. was deposited at relatively high sedimentation rates, and is partly coeval to healthy carbonate platforms. The low carbonate content of the Plattenkalke suggests that sedimentation rates were not primarily controlled by the sediment supply from the platform.

Sedimentological and geochemical evidence suggest aragonite dissolution contemporaneous with calcite precipitation at the water–sediment interface. As a consequence, episodes of strong aragonite dissolution resulted in non-sedimentation and dissolution at the sea floor leading to small hiatuses within the apparently continuous Livinallongo Fm. In addition, aragonite dissolution introduced a bias toward larger and thicker shelled ammonoids.

During deposition of the Knollenkalke Mb. the bottom water temperature was less than 10–15 °C. The base of this unit marks the arrival of cool water masses in the Dolomites and perhaps throughout the Southern Alps causing widespread aragonite dissolution on the sea floor. Coastal upwelling of these bottom waters is hypothesized to have started contemporaneously with the onset of Knollenkalke sedimentation, and may have caused the observed partial drowning and mud-mound nature of some Middle Triassic carbonate platforms of the Dolomites.

Carbon and oxygen stable isotope analyses of nodules, embedding sediments and late calcite veins in the Knollenkalke Mb. provide geochemical evidence of differential diagenesis. The  $\delta^{13}\text{C}$  values of calcite nodules of the Knollenkalke Mb. are regarded as proxies of the C isotopic composition of the bottom seawater.

In conclusion, we stress that western Tethys Triassic hemipelagites cannot be assumed to have deposited at constant sedimentation rates, unless careful sedimentologic, geochemical and/or stratigraphic investigations support such a statement. Hiatuses and condensation horizons are in fact to be expected.

## Acknowledgements

The authors wish to thank M. Rigo for providing CAI data; S. Furin and P. Fedele for the assistance in the field; F. Massari for fruitful discussions on the “Ammonitico Rosso”, M. Wimmer for assistance in the isotope lab. We acknowledge comments by L. Keim and an anonymous reviewer, as well as by editors F. Surlyk, F. Koning and B. Sellwood. Research funded by the MIUR, grant n° 2004048302 (resp. P. Mietto) and grant n° 2002045173 (resp. A. Bosellini).

## References

- Blendinger, W., 1994. The carbonate factory of Middle Triassic buildups in the Dolomites, Italy: a quantitative analysis. *Sedimentology* 41, 1147–1159.
- Blendinger, W., Parow, A., Keppler, F., 1982. Palaeogeography of the M. Cenera–Piz del Corvo area (Dolomites/Italy) during the Upper Anisian and Ladinian. *Geologica Romana* 21, 217–234.
- Blendinger, W., Brack, P., Norborg, A.K., Wulff-Pedersens, E., 2004. Three-dimensional modeling of an isolated carbonate buildup (Triassic, Dolomites, Italy). *Sedimentology* 51, 297–314.
- Bosellini, A., Ferri, R., 1980. La Formazione di Livinallongo (Buchenstein) nella valle di S. Lucano (Ladinico inferiore, Dolomiti bellunesi). *Annali dell'Università di Ferrara. Sezione. 9* 6, 63–89.
- Brack, P., Muttoni, G., 2000. High-resolution magnetostratigraphic and lithostratigraphic correlations in Middle Triassic pelagic carbonates from the Dolomites (northern Italy). *Palaeogeography, Palaeoclimatology, Palaeoecology* 161, 361–380.
- Brack, P., Rieber, H., 1986. Stratigraphy and ammonoids of the Lower Buchenstein Beds of the Brescian Prealps and Giudicarie and their significance for the Anisian/Ladinian boundary. *Eclogae Geologicae Helveticae* 79, 181–225.
- Brack, P., Rieber, H., 1993. Towards a better definition of the Anisian/Ladinian boundary: new biostratigraphic data and correlations of boundary sections from the Southern Alps. *Eclogae Geologicae Helveticae* 86, 415–527.
- Brack, P., Rieber, H., Nicora, A., 2003. The Global Stratigraphic Section and Point (GSSP) of the base of the Ladinian stage (Middle Triassic) – a proposal for the GSSP at the base of the Curionii Zone in the Bagolino section (Southern Alps, northern Italy). *Albertiana* 28, 13–25.
- Casati, P., Jadoul, F., Nicora, A., Marinelli, M., Fantini Sestini, N., Fois, E., 1982. Geologia della valle dell'Ansiei e dei gruppi Monte Popera-Tre Cime di Lavaredo (Dolomiti orientali). *Rivista Italiana di Paleontologia e Stratigrafia* 87, 371–510.
- Channell, J.E.T., Kozur, H.W., Sievers, T., Mock, R., Aubrecht, R., Sykora, M., 2003. Carnian–Norian biomagnetostratigraphy at Silická Brezová (Slovakia): correlation to other Tethyan sections and to the Newark Basin. *Palaeogeography, Palaeoclimatology, Palaeoecology* 191, 65–109.
- Cherns, L., Wright, V.P., 2000. Missing molluscs as evidence of large-scale, early skeletal aragonite dissolution in a Silurian sea. *Geology* 28, 791–794.
- Clari, P.A., Martire, L., 1996. Interplay of cementation, mechanical compaction, and chemical compaction in nodular limestones of the Rosso Ammonitico Veronese (Upper Jurassic, northeastern Italy). *Journal of Sedimentary Research* 66, 447–458.
- Cros, P., Houel, P., 1983. Repartition and paleogeographical interpretation of volcanoclastic and pelagic sediments of the Livinallongo Formation (Italian Dolomites). *Geologica et Palaeontologica. Mitteilungen Innsbruck* 11, 415–452.
- Cros, P., Vrielynck, B., 1989. Unconformity of pelagic limestones on dolomitic paleorelief at Piz del Corvo (Cenera Massif, Italian Dolomites, Northern Italy). *Stratigraphy and diagenesis. Neues Jahrbuch für Geologie und Paläontologie* 11, 641–655.
- De Zanche, V., Mietto, P., 1981. Review of the Triassic sequence of Recoaro (Italy) and related problems. *Rendiconti della Società Geologica Italiana* 4, 25–28.
- De Zanche, V., Gianolla, P., Mietto, P., Siorpaes, C., Vail, P.R., 1993. Triassic sequence stratigraphy in the Dolomites (Italy). *Memorie di Scienze Geologiche* 45, 1–27.
- De Zanche, V., Gianolla, P., Manfrin, S., Mietto, P., Roghi, G., 1995. A Middle Triassic backstepping carbonate platform in the Dolomites (Italy): sequence stratigraphy and biostratigraphy. *Memorie di Scienze Geologiche* 47, 135–155.
- Di Stefano, P., 1990. The Triassic of Sicily and Southern Apennines. *Bollettino della Società Geologica Italiana* 109, 21–37.
- Egenhoff, W., Peterhänsel, A., Bechstädt, T., Zühlke, R., Grötsch, J., 1999. Facies architecture of an isolated carbonate platform: tracing the cycles of the Latemär (Middle Triassic, northern Italy). *Sedimentology* 46, 893–912.
- Epstein, A.G., Epstein, J.B., Harris, L.D., 1977. Conodont color alteration — an index to organic metamorphism. *U.S. Geological Survey Professional Paper N°995* (27 pp.).
- Gawlick, H.-J., Böhm, F., 2000. Sequence and isotope stratigraphy of Late Triassic distal periplatform limestones from the Northern Calcareous Alps (Kälberstein Quarry, Berchtesgaden Hallstatt Zone). *International Journal of Earth Sciences* 89, 108–129.
- Gianolla, P., Jacquini, T., 1998. Triassic sequence stratigraphic framework of western European basins. Mesozoic and Cenozoic sequence stratigraphy of European Basins. *Special Publication - SEPM N°60*, 643–650.
- Goldhammer, R.K., Dunn, P.A., Hardie, L.A., 1987. High frequency glacio-eustatic sealevel oscillations with Milankovitch charac-

- teristics recorded in Middle Triassic platform carbonates in Northern Italy. *American Journal of Science* 287, 853–892.
- Kutzbach, J.E., Gallimore, R.G., 1989. Pangean climates: megamonsoons of the megacontinent. *Journal of Geophysical Research* D94, 3341–3357.
- Manfrin, S., Mietto, P., Preto, N., 2005. Ammonoid biostratigraphy of the Middle Triassic Latemar Platform (Dolomites, Italy) and its correlation with Nevada and Canada. *Geobios* 38, 477–504.
- Masetti, D., Neri, C., 1980. L'Anisico della Val di Fassa (Dolomiti Occidentali) sedimentologia e paleogeografia. *Annali dell'Università di Ferrara. Sezione 9* 7, 1–19.
- Maurer, F., Schlager, W., 2003. Lateral variations in sediment composition and bedding in Middle Triassic interplatform basins (Buchenstein Formation, Southern Alps, Italy). *Sedimentology* 50, 1–22.
- Maurer, F., Reijmer, J.J.G., Schlager, W., 2003. Quantification of input and compositional variations of calciturbidites in a Middle Triassic basinal succession (Seceda, Dolomites, Southern Alps). *International Journal of Earth Sciences* 92, 593–609.
- Mietto, P., Manfrin, S., 1995. A high resolution Middle Triassic ammonoid standard scale in the Tethys Realm. A preliminary report. *Bulletin de la Société Géologique de France* 166, 539–563.
- Mietto, P., Gianolla, P., Manfrin, S., Preto, N., 2003a. Refined ammonoid biostratigraphy of the Bagolino section (Lombardian Alps, Italy), GSSP candidate for the Anisian/Ladinian stage boundary. *Rivista Italiana di Paleontologia e Stratigrafia* 109, 449–462.
- Mietto, P., Manfrin, S., Preto, N., Gianolla, P., Krystyn, L., Roghi, G., 2003b. Proposal of the Global Stratigraphic Section and Point (GSSP) for the base of the Ladinian Stage (Middle Triassic) — GSSP at the base of the Avisianum Subzone (FAD of *Aplococeras avisianum*) in the Bagolino Section (Southern Alps, NE Italy). *Albertiana* 28, 26–34.
- Mojsisovics, E.M. Von, 1882. Die Cephalopoden der mediterranen Triasprovinz. *Abhandlungen der Kaiserlich Koniglichen Geologischen Reichsanstalt* 10, 1–332.
- Morse, J.W., Wang, Q., Tsio, M.Y., 1997. Influences of temperature and Mg:Ca ratio on CaCO<sub>3</sub> precipitates from seawater. *Geology* 25, 85–87.
- Munnecke, A., Westphal, H., Reijmer, J.J.G., Samtleben, C., 1997. Microspar development during early marine burial diagenesis: a comparison of Pliocene carbonates from the Bahamas with Silurian limestones from Gotland (Sweden). *Sedimentology* 44, 977–990.
- Muttoni, G., Kent, D.V., Di Stefano, P., Gullo, M., Nicora, A., Tait, J., Lowrie, W., 2001. Magnetostratigraphy and biostratigraphy of the Carnian/Norian boundary interval from the Pizzo Mondello section (Sicani Mountains, Sicily). *Palaeogeography, Palaeoclimatology, Palaeoecology* 166, 383–399.
- Muttoni, G., Nicora, A., Brack, P., Kent, D.V., 2004. Integrated Anisian/Ladinian boundary chronology. *Palaeogeography, Palaeoclimatology, Palaeoecology* 208, 85–102.
- Preto, N., Hinnov, L.A., Hardie, L.A., De Zanche, V., 2001. A Middle Triassic orbital signature recorded in the shallow-marine Latemar carbonate buildup (Dolomites, Italy). *Geology* 29, 1123–1126.
- Roberts, H.H., Rouse Jr., L.J., 1982. Cold water stress in Florida bay and northern Bahamas: a product of winter cold-air outbreaks. *Journal of Sedimentary Petrology* 52, 145–155.
- Scandone, P., 1967. Studi sulla geologia lucana: la serie silicomarmosa e i suoi rapporti con l'Appennino calcareo. *Bollettino della Società Naturalistica di Napoli* 76, 1–175.
- Schlager, W., 1974. Preservation of cephalopod skeletons and carbonate dissolution on ancient Tethyan sea floors. In: Hsü, K.J., Jenkins, H.C. (Eds.), *Pelagic Sediments: On Land and Under the Sea*. International Association of Sedimentologists Special Publication No 1, pp. 49–70.
- Spötl, C., Vennemann, T.W., 2003. Continuous-flow isotope ratio mass spectrometric analysis of carbonate minerals. *Rapid Communications in Mass Spectrometry* 17, 1004–1006.
- Stanley, S.M., Hardie, L.A., 1998. Secular oscillations in the carbonate mineralogy of reef-building and sediment-producing organisms driven by tectonically forced shifts in seawater chemistry. *Palaeogeography, Palaeoclimatology, Palaeoecology* 144, 3–19.
- Veizer, J., Ala, D., Azmy, K., Bruckschen, P., Buhl, D., Bruhn, F., Carden, G.A.F., Diener, A., Ebner, S., Godderis, Y., Jasper, T., Korte, C., Pawellek, F., Podlaha, O.G., Strauss, H., 1999. <sup>87</sup>Sr/<sup>86</sup>Sr,  $\delta^{13}\text{C}$  and  $\delta^{18}\text{O}$  evolution of Phanerozoic seawater. *Chemical Geology* 161, 59–88.
- Viel, G., 1979. Litostratigrafia ladinica: una revisione. Ricostruzione paleogeografica e strutturale dell'area Dolomitico-Cadorina (Alpi Meridionali). *Rivista Italiana di Paleontologia e Stratigrafia* 85, 85–125.
- Vörös, A., Szabó, I., Kovács, S., Dosztály, L., Budai, T., 1996. The Felsőörs section: a possible stratotype for the base of the Ladinian stage. *Albertiana* 17, 25–40.
- Wright, V.P., 1994. Early Carboniferous carbonate systems; an alternative to the Cainozoic paradigm. *Sedimentary Geology* 93, 1–5.
- Wright, V.P., Chems, L., Hodges, P., 2003. Missing molluscs: field testing taphonomic loss in the Mesozoic through early large-scale aragonite dissolution. *Geology* 31, 211–214.
- Zühle, R., Bechstädt, T., Mundil, R., 2003. Sub-Milankovitch and Milankovitch forcing on a model carbonate platform — the Latemar (Middle Triassic, Italy). *Terra Nova* 15, 69–80.